

# iTRAQ-based proteomic analysis of duck muscle related to lipid oxidation

Muhan Zhang,<sup>\*,†</sup> Daoying Wang,<sup>†</sup> Xinglian Xu,<sup>\*,1</sup> Weimin Xu,<sup>†</sup> and Guanghong Zhou<sup>†</sup>

*\*Key Lab of Meat Processing and Quality Control, Ministry of Education, Nanjing Agricultural University, Nanjing 210095, PR China; and <sup>†</sup>Institute of Agricultural Products Processing, Jiangsu Academy of Agricultural Sciences, Nanjing 210014, PR China*

**ABSTRACT** Lipid oxidation is the main cause of quality deterioration in meat and meat products. To facilitate the identification of candidate molecular biomarkers that are linked to lipid oxidation, we performed the proteomic analysis of duck muscle using isobaric tag for relative and absolute quantification (**iTRAQ**), followed by parallel reaction monitoring (**PRM**) to confirm the iTRAQ results. *Pectoralis major* muscles were divided into 2 groups in accordance with lipid oxidation,

and iTRAQ-based analysis identified a total of 301 differentially expressed proteins, of which 15 proteins were examined by PRM assay. Proteins involved in lipid binding and metabolism, lipolysis, stress response, oxidative respiratory chain, and redox regulation were found to be differentially expressed between 2 groups and might affect lipid oxidation in muscles. The findings could contribute to the improved understanding of key proteins and processes engaged in lipid oxidation of meat.

**Key words:** proteomics, iTRAQ, lipid oxidation

2021 Poultry Science 100:101029

<https://doi.org/10.1016/j.psj.2021.101029>

## INTRODUCTION

Lipid oxidation is a major cause of quality deterioration in meat products; it also causes loss of nutritional values and generates compounds that may pose risks to human health (Domínguez et al., 2019). Lipid oxidation starts immediately after slaughtering, and occurs through a free radical chain reaction including reactive oxygen species (**ROS**) and reactive nitrogen species, or nonradical reactions involving enzymes (Amaral et al., 2018). The rate and extent of lipid oxidation in muscle is determined by preslaughtering events such as oxidative stress and postslaughtering muscle metabolism that affect the balance between pro-oxidants and antioxidants (Amaral et al., 2018). The degree of lipid oxidation could be varied among different species, muscle types, and individuals, and multiple processes and environmental conditions could affect the oxidative status of meat (Amaral et al., 2018). Understanding the complex biochemical processes linked to the lipid oxidation in different

muscles could provide a basis for explaining quality variability and predicting meat quality.

Proteins are major components of meat involved in complex biochemical and physiological changes that may alter meat quality attributes, and they are closely related to lipid oxidation (Guyon et al., 2016). Meat contains a number of endogenous antioxidants including the antioxidant enzymes, peptides, and proteins, functioning as metal ion chelators or free radical scavengers; it also contains enzymes and proteins that could initiate lipid peroxidation by generation of radicals or release of metal ions (Domínguez et al., 2019). Proteomics has great potential to discover biomarkers associated with lipid oxidation to reduce meat quality variability and facilitate preslaughter and postslaughter handling of animals. Sayd et al. (2012) used 2D electrophoresis in combination with liquid chromatography–tandem mass spectrometry (**LC-MS/MS**) to analyze the proteome related to lipid oxidation of pork at various aging times and after cooking. Redoxin enzymes, annexins, and proteins involved in lipid transporters and aerobic respiration have been identified to be related with lipid oxidation among different storage and cooking times. However, the differentially expressed proteins between different lipid oxidation degree groups have been minimally investigated.

Isobaric tag for relative and absolute quantification (**iTRAQ**) is one of the most sensitive techniques

© 2021 Published by Elsevier Inc. on behalf of Poultry Science Association Inc. This is an open access article under the CC BY-NC-ND license (<http://creativecommons.org/licenses/by-nc-nd/4.0/>).

Received July 16, 2020.

Accepted January 19, 2021.

<sup>1</sup>Corresponding author: [xlxu@njau.edu.cn](mailto:xlxu@njau.edu.cn)

currently used for quantitative analysis of proteomes, which is more reliable than the traditional 2D electrophoresis (Karp et al., 2010). Parallel reaction monitoring (PRM) is a recent development in targeted mass spectrometry, which involves the use of quadrupole-equipped Orbitrap. This method is more specific and sensitive than selected reaction monitoring and has been widely used to quantify and detect target proteins (Tsuchiya et al., 2013).

Duck meat is particularly susceptible to oxidative damage owing to its high degree of lipid unsaturation (Wang et al., 2009). It is well accepted by consumers in China, and about thirty million ducks are consumed annually in Nanjing city alone (Liu et al., 2006). In this study, the differentially expressed proteins in duck muscles between high and low lipid oxidation groups were analyzed by iTRAQ, and PRM was used to confirm the iTRAQ results. The aim of the present study was to find the associations between lipid oxidation and proteome profiles of duck muscle and to suggest possible mechanisms in the development of meat quality traits.

## MATERIALS AND METHODS

### Sample Preparation

Twenty-four lean-type Cherry Valley ducks with the average weight of 1.5 kg were obtained from a commercial processing plant where they were slaughtered by bleeding from a unilateral neck cut severing the left carotid artery and jugular vein (Jiangsu Yurun Food Ltd., Nanjing, China). Two skinless, deboned breast fillets (*Pectoralis major*) were taken immediately from each carcass and placed into a plastic bag on ice, and the fillets from the same carcass were considered as one biological replicates. The meat was trimmed from visible fat and connective tissue, around 10 g muscles were cut and measured for pH at 45 min postmortem, and 10 g were collected and snap-frozen in liquid nitrogen for the extraction of total proteins. The residual muscle was subjected to other measurements on the sampling day after the measurement of initial pH. Lipid oxidation and morphology was evaluated after 3 d of refrigerated storage in the dark in plastic bags. All measurements were performed in triplicate.

### Cooking Loss and Shear Force

Each sample was weighed accurately before cooking. The sample in a polyethylene cooking bag was immersed in an 80°C water bath until reaching an internal end point of 75°C. After cooking, the sample was cooled to the internal temperature of room temperature and wiped with blotting paper to remove excess water, followed by weighing immediately. Cooking loss was calculated as, cooking loss (%) = [(raw weight - cooked weight)/raw weight] × 100.

After measuring cooking loss, the same muscle was then used for the determination of shear force. Shear force was determined through the application of the

Meullenet-Owens razor shear test (Meullenet et al., 2004), using a texture analyzer (TVT-300XP; TexVol Instruments, Viken, Sweden) equipped with a razor blade with a height of 24 mm and a width of 8.9 mm. Muscle strips were cut across the fiber axis. The crosshead speed was set at 2 mm/s, and the test was triggered by a 10 g contact force. The shear was perpendicular to the axis of muscle fibers.

### pH Value

Two grams of muscle, taken at 45 min, was homogenized at 5,000 rpm with an Ultra Turrax homogenizer (T25, IKA, Labortechnik, Staufen, Germany) in 18 mL distilled water, and the pH of the homogenate was measured using a pH meter equipped with an electrode (FE-20; Mettler Toledo, Shanghai, China).

### Meat Color

The meat color ( $L^*$ ,  $a^*$ , and  $b^*$ ) was measured using a Colorimeter (CR 400, Minolta, Osaka, Japan). The colorimeter was calibrated using a standard white ceramic tile before measuring samples.

### Determination of Thiobarbituric Acid Reactive Substances

Lipid oxidation of all samples was measured by the 2-thiobarbituric (TBA) method according to Sorensen and Jorgensen (1996). Two grams of sample was homogenized with 10 mL of a 7.5% trichloroacetic acid solution containing 0.1% propyl gallate and 0.1% ethylenediaminetetraacetic acid disodium salt for 30 s in an Ultra Turrax blender (9,500 rpm) and filtered through a Whatman filter No. 42. Equal 5 mL volumes of filtrate and 0.02 mol TBA solution were mixed with glass stopped tubes and incubated in a water bath at 100°C for 40 min before cooling to room temperature under running cold tap water. The absorbance was measured at 532 nm using a spectrophotometer. Thiobarbituric acid reactive substances was calculated from a standard curve of malondialdehyde (MDA), freshly prepared by acidification of 1,1,3,3-tetraethoxypropane in the range from 0.02 µg/mL to 0.3 µg/mL and expressed as mg of MDA per kg sample.

### ROS and NO Detection

2,7-Dichlorofluorescein diacetate (DCFH-DA) and 4-amino-5-methylamino-2',7'-difluorofluorescein diacetate (DAF-FM DA) were used as chemical probes for ROS and nitric oxide (NO) measurement, respectively (Kang et al., 2009). Approximately 2 g of frozen muscles from each sample were crushed and homogenized on ice in 20 mL of Tris-HCl buffer (100 mmol Tris-HCl, pH 8.0) and a protease inhibitors cocktail (Sigma-Aldrich Corp., St. Louis, MO) followed by centrifugation at 12,000 g for 10 min at 4°C. DCFH-DA or DAF-FM DA was mixed with muscle extract at the final concentration of

10  $\mu\text{M}$  and 5  $\mu\text{M}$  respectively, and they were incubated at 37°C for 30 min. The fluorescence intensity was measured at 485 and 525 nm for ROS, and 500 and 515 nm for NO as the respective excitation wavelength and emission wavelength on a Cytation5 microplate reader (BioTek Instruments Inc., Winooski, VT). The probe alone was used as a negative control, and the baseline fluorescence was the sample without the probe. Data were expressed as the fluorescence of the sample after deduction of the negative control and baseline fluorescence.

### **Muscle Specimen Preparation and Hematoxylin and Eosin Staining**

Muscle tissues were sliced into 1-4 mm sections behind the optic chiasma and were subsequently fixed in 4% paraformaldehyde at 4°C according to [Xiao et al. \(2017\)](#) with modifications. The sections were then dehydrated in a dehydration box. Melted paraffin was poured into the embedding box, followed by the muscle sections. When the paraffin was completely hardened, the paraffin block was removed from the embedding box and stored at 4°C. For slicing, the paraffin block was placed on a paraffin slicing machine and sectioned from the front to the back to make 4  $\mu\text{m}$  thick sections. The slices, which floated on the surface, were flattened and lifted onto the slides. The sections were then placed in a 60°C incubator overnight.

### **iTRAQ Assays**

The duck muscles were segregated into high and low MDA groups, with 3 samples randomly selected in each group. Each sample was ground in liquid nitrogen and suspended in lysis buffer consisting of 8 mol urea (U5378; Sigma), 100 mmol Tris-HCl (pH 8.0), 10 mmol dithiothreitol (DTT), and proteinase inhibitors (4693116001; Roche). About 200  $\mu\text{g}$  protein was added to 5  $\mu\text{L}$  of 1 mol DTT at 37°C for 1 h and alkylated with 20  $\mu\text{L}$  of 1 mol indole acetic acid at room temperature for 1 h in the dark. Trypsin digestion (protein:trypsin ratio of 20:1) was performed for more than 12 h at 37°C.

The samples were labeled as per the instructions of iTRAQ Reagent-8plex Multiplex Kit (AB SCIEX). Protein samples were labeled as 113-119 and 121, and then pooled and dried by centrifugal evaporation. The peptides were further fractionated using a Gemini C18 column (4.6  $\times$  250 mm, 5  $\mu\text{m}$ ) on Shimadzu LC-20AB liquid-phase system. The peptides were dissolved in mobile phase A (5% ACN, pH 9.8) and eluted at a flow rate of 1 mL/min with the following gradient: 5% mobile phase B (95% ACN, pH 9.8) for 10 min, 5% to 35% mobile phase B for 40 min, 35% to 95% mobile phase B for 1 min, mobile phase B for 3 min, and 5% mobile phase B for 10 min. The elution peak was monitored at a wavelength of 214 nm and one component was collected per minute.

Chromatography and tandem mass spectrometry of the tryptic peptides was performed on a Q-Exactive Orbitrap HF mass spectrometer (Thermo Scientific). The samples were separated at a flow rate of 300 nL/min using a C18 column (Thermo Scientific, 0.75 $\times$ 250 mm, 3  $\mu\text{m}$ ) with mobile phase A (2% ACN, 0.1% formic acid) and B (98% acetonitrile, 0.1% formic acid). The gradient elution program was as follows: 0-5 Min, 5% mobile phase B; 5-45 min, mobile phase B linearly increased from 5% to 25%; 45-50 min, mobile phase B increased from 25% to 35%; 50-52 min, mobile phase B rose from 35% to 80%; 52-54 min, 80% mobile phase B; 54-60 min, 5% mobile phase B. The nano-liter liquid-phase separation end was directly connected to the mass spectrometer. The main parameters were set: ion source voltage was set to 1.9 kV, MS1 scanning range was 350-1,500 m/z; resolution was set to 60,000; MS2 starting m/z was fixed at 100; resolution was 15,000. The ion screening conditions for MS2 fragmentation: charge 2+ to 6+, and the top 20 parent ions with the peak intensity exceeding 10,000. The ion fragmentation mode was HCD, and the fragment ions were detected in Orbitrap.

The Mascot and Proteome Discoverer (Thermo Scientific) were used for raw data file processing and protein identification. The peptide mass tolerance was  $\pm 15$  ppm, and fragment mass tolerance was 20 mmu. Proteins were quantified based on the peptides allocated to the respective protein. Fold change of  $\geq 1.2$  or  $\leq 0.83$  was set as the threshold to identify differently expressed proteins.

### **PRM-MS Analysis**

The protein expression levels obtained using iTRAQ was confirmed by quantifying the expression levels of proteins by a PRM-MS analysis. Each precursor ion was selected by the quadrupole, fragmented, and then all fragment ions were quantified on Q-Exactive Orbitrap HF mass spectrometer (Thermo Scientific). The sum of the top 5 fragment ion intensities was calculated in Skyline (MacCoss Lab Software version 3.6.1.10556) and used to estimate peptide signal intensity. Peptide concentration was calculated based on the ratio to the heavy peptide standards that were added in known quantity.

### **Bioinformatics and Statistical Analysis**

Gene ontology terms were enriched through division in 3 subcategories that include cellular component, molecular function, and biological process using Blast2GO software (<http://www.blast2go.org>). The functional interactions between the identified proteins were performed using String software.

Statistical analysis of the differences between each group was evaluated by one-way analysis of variance using the SPSS 18.0 and values of  $P < 0.05$  was considered as statistically significant.

## RESULTS AND DISCUSSION

### Meat Quality Characteristics

The meat quality attributes of the duck classified in 2 groups with significant differences in lipid oxidation are shown in [Table 1](#). The muscles were segmented into low (MDA < 0.25 mg/kg) and high MDA (MDA > 0.45 mg/kg) groups. The muscles in the high MDA group exhibited lower pH and shear force, and had higher lightness and cooking loss than those in the low MDA group, but there was no significant difference ( $P > 0.05$ ).

The generation of ROS and NO in each group was examined via the DCFH-DA and DAF-FM DA probe, respectively ([Figure 1](#)). As expected, the production of ROS and NO in high MDA group was significantly higher than that in low MDA group ( $P < 0.05$ ), suggesting the radicals are probably responsible for the progression of lipid oxidation in meat. Reactive oxygen species and reactive nitrogen species such as hydroxyl radical ( $\bullet\text{OH}$ ), superoxide anion ( $\text{O}_2^-$ ), hydrogen peroxide ( $\text{H}_2\text{O}_2$ ), and nitric oxide (NO) are highly reactive to initiate lipid oxidation ([Amaral et al., 2018](#)). It was proposed that endogenous enzymes are potential sources of ROS and NO in muscle fiber cytosol, and electron spin resonance analysis revealed that protein-derived radicals, rather than the iron-derived radicals, were generated during high pressure treatment of muscles and initiated lipid oxidation ([Bolumar et al., 2014](#)). Myoglobin, xanthine oxidase, and enzymes of fatty acid metabolism including cyclooxygenases and lipoxygenases have been identified as potential sources of ROS in the muscle ([Murrant and Reid, 2001](#)).

The microstructure of meat samples was observed longitudinally and transversally with HE staining and light microscopy as shown in [Figure 2](#). The muscle fibers of low MDA group muscle were more intact and compact than that in the high MDA group. The low MDA group muscle displayed only small spaces, whereas the high MDA group muscle appeared very loose and severe damaged with larger drip channels along the muscle fiber direction. Oxidation is a leading cause for quality deterioration of meat ([Domínguez et al., 2019](#)). As intramuscular and membrane phospholipids contain unsaturated fatty acids, and oxygen and some free radicals are more soluble in the fluid lipid bilayer than in the aqueous solution, the phospholipids are extremely

sensitive to oxidation ([Pamplona, 2008](#)). Phospholipid oxidation could lead to the degradation of biological membranes and consequently to the loss of membrane integrity and functions, as a result, the cell is disrupted ([Pamplona, 2008](#)). Diffusion of oxidative species from the membrane to the interior could subsequently oxidize sarcoplasmic and myofibrillar proteins, causing damage to the cells and tissues and textural changes ([Guyon et al., 2016](#)).

### Comparative Proteomic Analysis

An 8-plex LC-MS/MS analysis produced 977,589 spectra, corresponded to 14,077 unique peptides, and 3,899 proteins were identified at a false discovery rate of  $\leq 0.01$ . About 49% of the identified proteins had 2 or more unique peptides. A total of 301 proteins were significantly different in expression levels between low and high MDA groups, as shown in [Supplementary Table 1](#).

The PRM assay was used to validate the differentially expressed proteins identified in iTRAQ analysis. The expression levels of the upregulated proteins were higher and those of the downregulated proteins were lower, in agreement with the findings of the iTRAQ analysis ([Table 2](#)). Parallel reaction monitoring uses targeted tandem MS to simultaneously monitor product ions of a targeted peptide with high resolution, mass accuracy, and reproducibility. In brief, the precursor ion of interest is isolated by the quadrupole and fragmented in the high-energy collisional dissociation cell, then the fragment ions are analyzed with an Orbitrap mass analyzer ([Ronsein et al., 2015](#)). Because of this parallel monitoring, there is no need for prior selection of target peptide transitions. Moreover, PRM offers higher specificity because it monitors product ions with high resolution and is therefore less likely to be affected by interfering ions ([Ronsein et al., 2015](#)).

Adipocyte-like fatty acid-binding protein (A-FABP) and apolipoprotein C-III are involved in lipid binding, transport, and metabolism, and they were identified to be more abundant in the high MDA group. The present result was consistent with the study by [Sayd et al. \(2012\)](#) that FABP was positively correlated with lipid oxidation in pork during storage. [Jurie et al. \(2007\)](#) have also reported that the expression of A-FABP was greater in oxidative muscle and it was a relevant indicator of marbling in cattle. The function of FABP is to deliver oxidized fatty acids to the nucleus and to bind and protect polyunsaturated fatty acids from oxidation ([Mentzer et al., 2001](#)), the accumulation of oxidized fatty acids may induce the elevated expression of FABP that facilitate the transport and catabolism of fatty acids in skeletal muscle.

It could be noted that cytosolic phospholipase A<sub>2</sub> (cPLA<sub>2</sub>) expression level was higher in low MDA group. PLA<sub>2</sub>, a calcium-dependent enzyme, cleaves phospholipids at the sn-2 position to give free fatty acids and lysophospholipids. Phospholipids are the major components of intramuscular lipid and cell membrane and contain large proportions of polyunsaturated fatty acids,

**Table 1.** Quality characteristic of duck muscles in high and low MDA groups.

Trait	High MDA (n = 3)	Low MDA (n = 3)
MDA (mg/kg)	0.48 ± 0.04 <sup>a</sup>	0.21 ± 0.03 <sup>b</sup>
pH	5.92 ± 0.06 <sup>a</sup>	6.04 ± 0.10 <sup>a</sup>
L*	45.20 ± 2.75 <sup>a</sup>	44.23 ± 4.74 <sup>a</sup>
a*	12.77 ± 3.24 <sup>a</sup>	15.48 ± 3.68 <sup>a</sup>
b*	0.97 ± 0.82 <sup>a</sup>	2.13 ± 1.42 <sup>a</sup>
Cooking loss (%)	19.11 ± 2.81 <sup>a</sup>	15.89 ± 3.76 <sup>a</sup>
Shear force (kg)	1.53 ± 0.32 <sup>a</sup>	1.67 ± 0.18 <sup>a</sup>

Data are expressed as the mean ± standard deviation.

In a row, values with different superscript differ significantly ( $P < 0.05$ ).

Abbreviation: MDA, malondialdehyde.

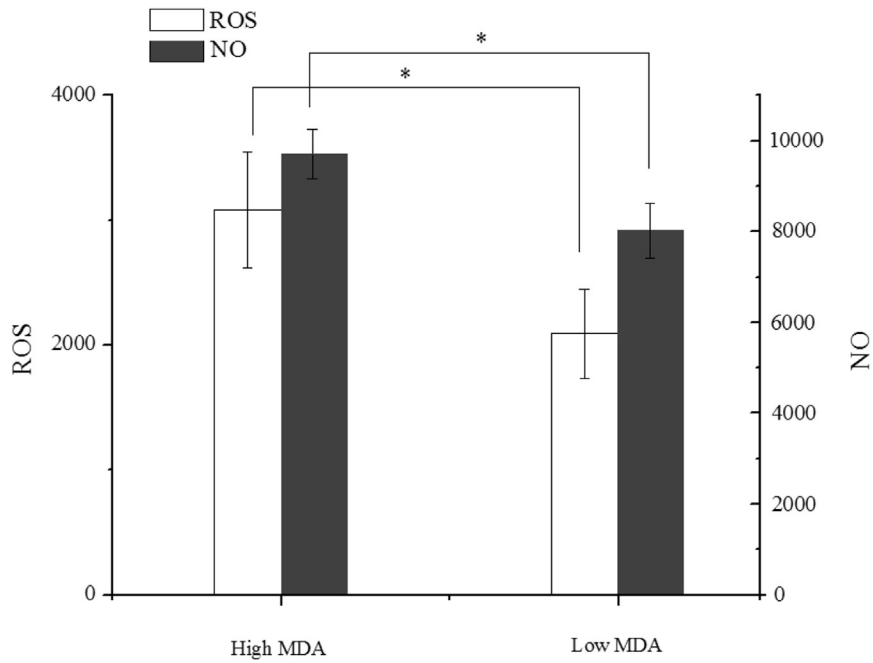


**Figure 1.** Reactive oxygen species (ROS) and NO generation in high and low MDA grouped muscles. \* $P < 0.05$ . Abbreviations: NO, nitric oxide; MDA, malondialdehyde.

which make them very susceptible to oxidative attack. It is usually considered that PLA<sub>2</sub> contributes indirectly to the lipid oxidation by releasing free fatty acids, which is then oxidative metabolized by lipoxygenase and cyclooxygenase (Adibhatla and Hatcher, 2006). However, in the study by Tatiyaborworntham and Richards (2015), the effect of PLA<sub>2</sub> on lipid oxidation was shown to be species dependent, which was antioxidant in cod and pork muscles but pro-oxidative in chicken muscles. The

lipid oxidation may also depend on the type of PLA<sub>2</sub>, calcium-independent phospholipase A<sub>2</sub> (iPLA<sub>2</sub>) activity was found to be correlated with lipid oxidation in PSE pork, whereas cPLA<sub>2</sub> activity had no significant difference between PSE and normal meat (Chen et al., 2010).

Selenoprotein S and thioredoxin were identified to be downregulated in low MDA group muscles. Selenoproteins are redox enzymes containing at least one selenocysteine, families of selenoproteins include

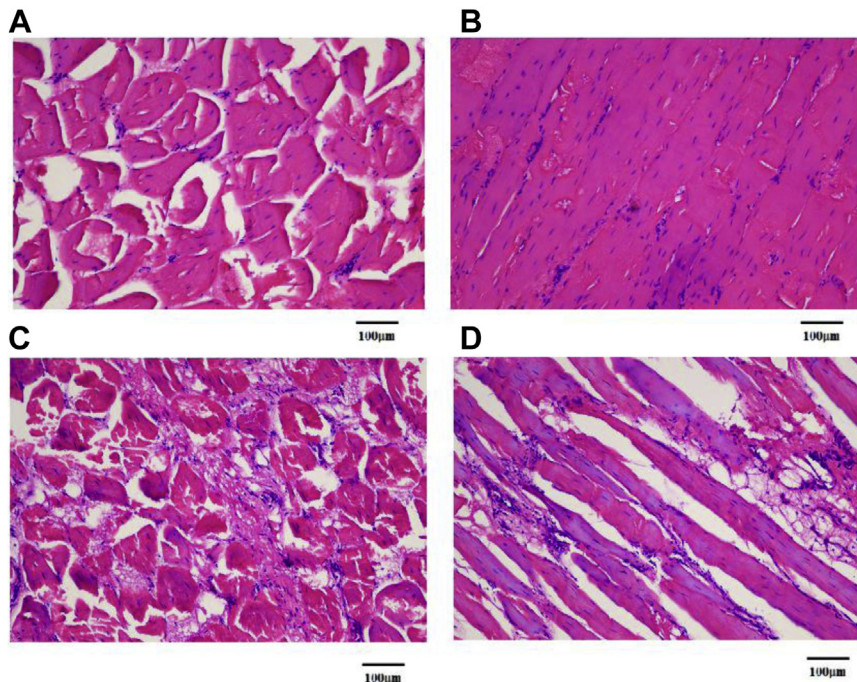


**Figure 2.** Hematoxylin and eosin staining of the duck muscles. A and B: transversal and longitudinal sections of muscle in low MDA group, C and D: transversal and longitudinal sections of muscle in high MDA group. Nuclei of cells are colored in blue (hematoxylin) and cytoplasm is colored in red (eosin). Abbreviation: MDA, malondialdehyde.

**Table 2.** Confirmation of differentially expressed proteins using PRM analysis.

Accession	Description	A/B fold change in PRM	A/B fold change in iTRAQ
XP_012957009.1	Cytosolic phospholipase A2 zeta isoform X3	1.47	1.33
XP_013043040.1	NADH dehydrogenase	1.26	1.24
NP_001297288.1	Myosin light chain 1, skeletal muscle isoform	1.44	1.26
EOB05436.1	Cytoskeleton-associated protein 5	1.63	1.5
EOB05903.1	Choline transporter-like protein	1.33	1.42
XP_013028005.1	Fatty acid-binding protein, adipocyte-like	0.77	0.81
EOB02816.1	Oxysterol-binding protein-related protein 11	0.65	0.82
EOB07468.1	Selenoprotein S	0.76	0.81
NP_001297295.1	Alpha-crystallin B chain	0.79	0.71
EOA92904.1	Stress-induced phosphoprotein 1	0.80	0.77
XP_013049614.1	Actin	0.63	0.5
OXB72919.1	Thioredoxin	0.72	0.83
XP_027313959.1	Heat shock protein HSP 90-alpha	0.81	0.82
NP_001289056.1	Apolipoprotein C-III	0.75	0.8
EOA95011.1	Aldehyde oxidase	0.55	0.62
AFA50437.1	Hemoglobin alpha D subunit	0.67	0.72

A is low MDA group, B is high MDA group, n = 3 in each group.

Abbreviations: iTRAQ, isobaric tag for relative and absolute quantification; MDA, malondialdehyde; PRM, parallel reaction monitoring

glutathione peroxidases, iodothyronine deiodinases, thioredoxin reductases, selenoprotein P, selenoprotein S, selenoprotein O and so on (Burk et al., 2003). They have pivotal significance for animal health due to their antioxidant activity, and their antioxidative abilities in the removal of radicals and hydroperoxides, repair of damaged molecules and regulation of many redox signaling events caused by oxidative stress have been well described (Benhar, 2018; Zoidis et al., 2018). The thioredoxin system, comprising NADPH, thioredoxin reductases, and thioredoxin, is a major antioxidant system defense against oxidative stress through its disulfide reductase activity regulating protein dithiol/disulfide balance (Lu and Holmgren, 2014). Thioredoxin plays critical roles in the adipogenesis, immune response, and cell death via interacting with other proteins (Chutkow and Lee, 2011). The thioredoxin system together with selenoproteins could control the cellular redox environment and serve as a backup system for each other (Lu and Holmgren, 2014). The expression of selenoproteins and thioredoxin could be activated and increased in response to oxidative stress, which might explain the correlation between higher protein levels and higher degree of lipid oxidation, and the present results with other studies imply they could probably be used as markers of oxidative stress (Lu and Holmgren, 2014; Zoidis et al., 2018).

Hemoglobin (**Hb**) is one of the most abundant proteins in animal muscles; it had increased expression in high MDA grouped muscles as compared with low MDA grouped muscles. Hemoglobin consists of 4 polypeptide chains with each chain containing one porphyrin heme moiety, the latter containing an iron atom that exist in a reduced (ferrous) or oxidized (ferric) form coordinated inside the heme ring (Grunwald and Richards, 2006). During storage and processing of muscles, Hb autooxidation, ferryl radical formation, heme dissociation, heme destruction, and iron release can all occur in

a very short time sequence and simultaneously, they have been recognized as major promoters of lipid oxidation (Grunwald and Richards, 2006; Wu et al., 2017). The greater expression of Hb might result in more rapid lipid oxidation in high MDA grouped muscles.

Stress-induced phosphoprotein 1, heat shock protein 90-alpha (Hsp90) and alpha-crystallin B chain were shown to be positively correlated with lipid oxidation. They are either expressed constitutively or inductively in response to stress to regulate cellular homeostasis and promote cell survival (Kalmar and Greensmith, 2009). They could directly protect lipid and cells against ROS-induced lipid oxidation, regulate apoptosis through multiple signaling pathways, and repair and modulate a number of chaperone proteins such as glutathione peroxidases, acting as important contributors to the cellular defense mechanism against oxidative stress (Christopher et al., 2014; Zhang et al., 2018b). In addition, Hsp90 and alpha-crystallin have been reported to bind with phospholipids and maintain the integrity and stability of membranes (Tsvetkova et al., 2002; Zhang et al., 2018a). Membrane lipid oxidation could lead to loss of membrane integrity and function as discussed above, whereas Hsps are upregulated in oxidative stress and have beneficial effects in the maintenance of the integrity and function of membrane phospholipids (Pamplona, 2008).

NADH dehydrogenase is an important complex in the mitochondrial oxidative respiratory chain, and energy production and metabolism. It was upregulated in low MDA group muscles, suggesting the increased level of NADH dehydrogenase may relate to decreased lipid oxidation in muscles. There has been no evidence of the role of NADH dehydrogenase on the intramuscular lipid oxidation and meat quality, but several studies showed it plays an important role in oxidative stress and ROS production in cells (Pelin et al., 2018; Murali et al., 2020).

### Bioinformatics Analysis

The differentially expressed proteins identified by iTRAQ were classified using the Gene Ontology categories (Figure 3). The cellular component analysis

revealed that the main protein localization was cell, cell part, organelle, and membrane. The molecular function indicated most proteins participated in cellular process, metabolic process, and biological regulation. The biological process analysis showed that the proteins were

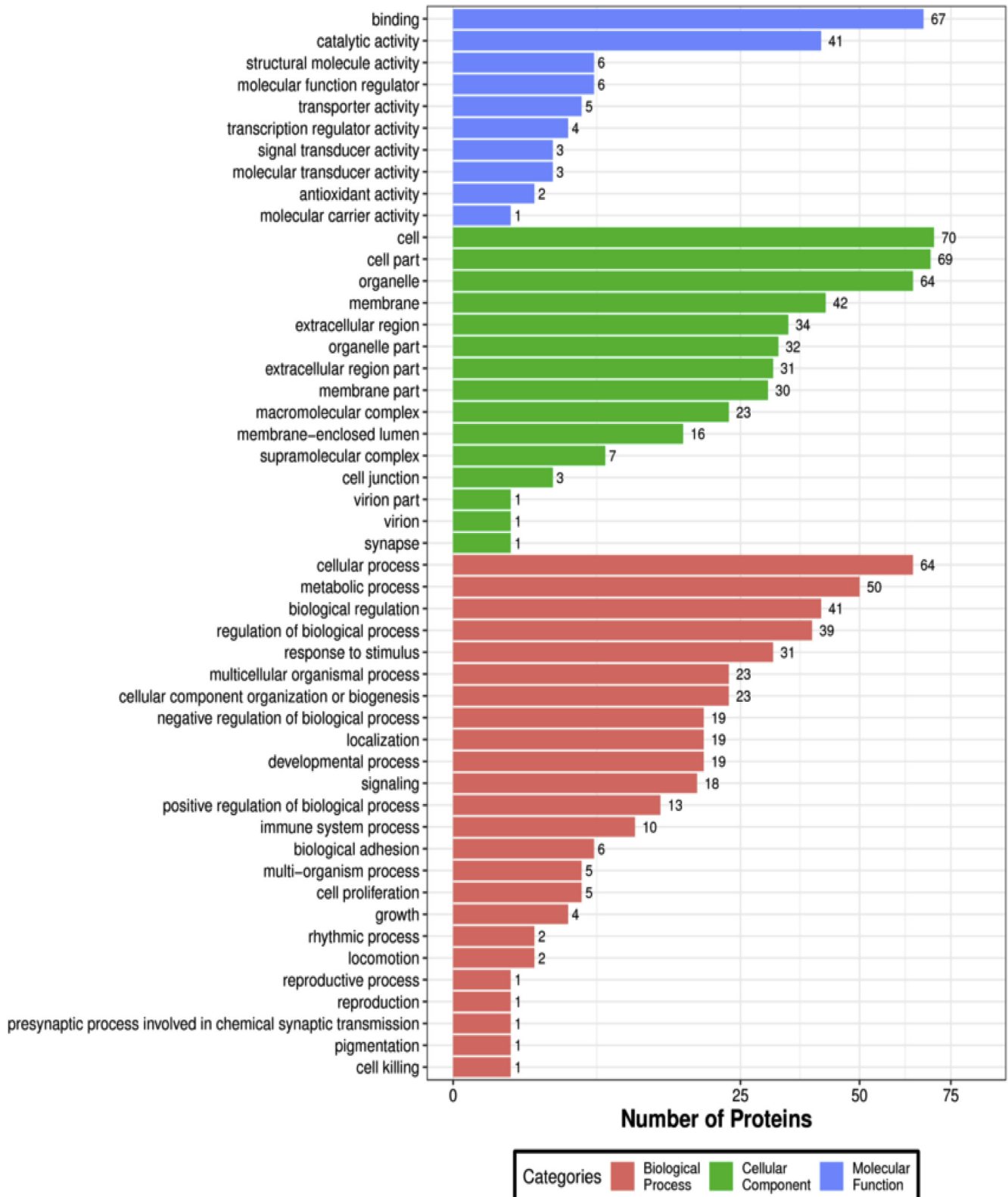


Figure 3. Classification of differential expressed proteins identified by GO functional classification.

mainly involved in binding, catalytic activity, structural molecule activity, and molecular function regulator.

Strong interactions were found among the differentially expressed proteins related to lipid oxidation by searching the String database (Figure 4). Structural proteins (actin, myosin light chain 1), redox regulation-related proteins (thioredoxin), stress proteins (Hsp90, alpha-crystallin B chain), and proteins involved in oxidative respiratory chain (NADH dehydrogenase) had more than 10 interactions with other proteins and plays pivotal roles in the interaction network. These proteins with different functions and locations may not exist independently, and they function together in the whole regulatory network to mediate lipid oxidation in the muscle.

## CONCLUSIONS

In summary, this study gives a better understanding of proteome associated with lipid oxidation in duck muscle. A-FABP, apolipoprotein C-III, cPLA<sub>2</sub>, Hb, selenoprotein S, thioredoxin, stress proteins, and NADH dehydrogenase exhibited differential expression between low and high MDA groups, which might correlate with the varied radical production and structural changes of meat. The bioinformatics analysis further showed that differentially expressed proteins were mainly involved in binding, catalytic activity, structural molecule activity, and molecular function regulator. Some significant findings may serve as clues to predict and regulate lipid oxidation in meat in the future.

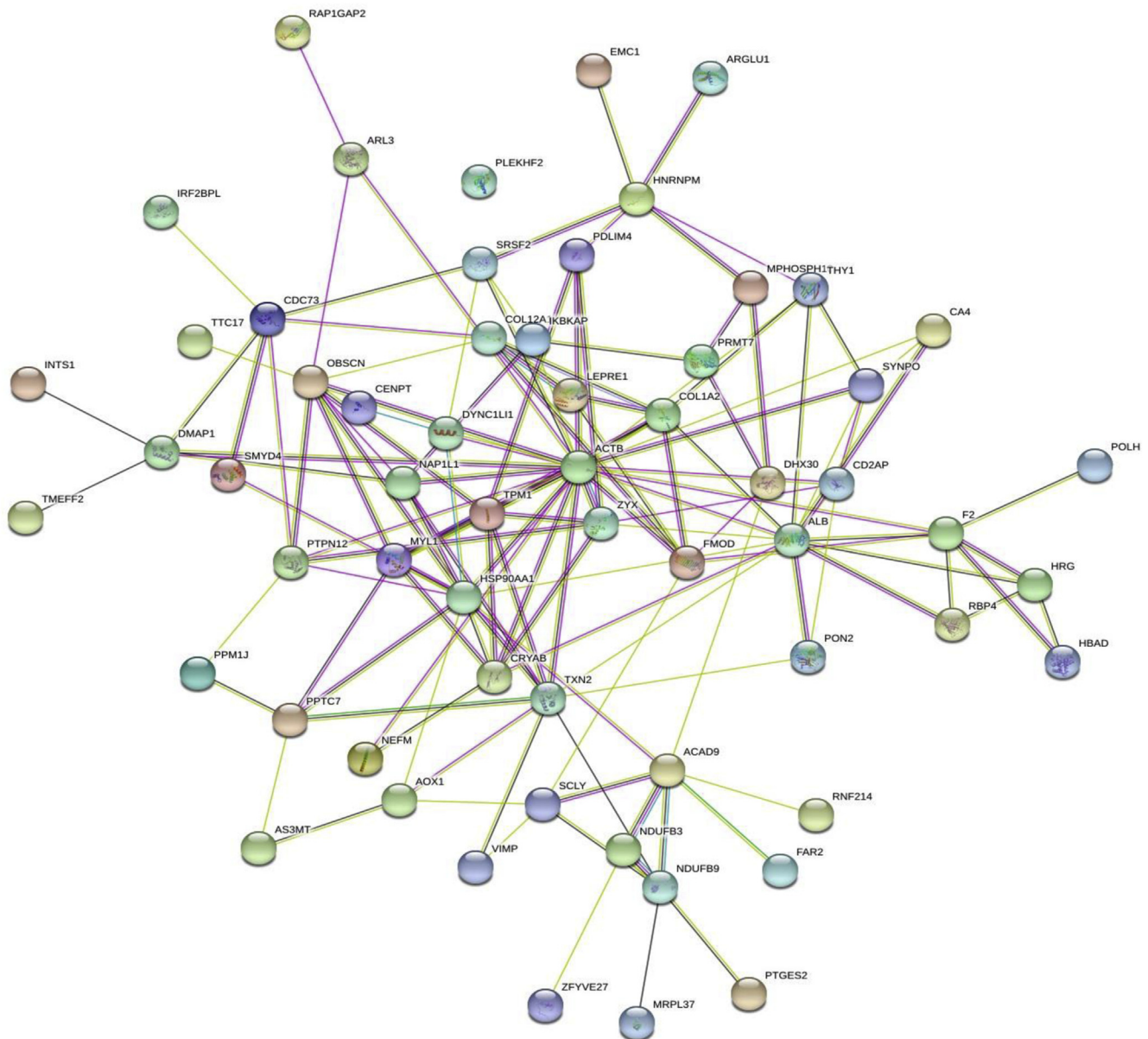


**Figure 4.** Interaction network of differential abundance proteins. The nodes were proteins from *Gallus gallus* database and the lines were the functional annotations. A light blue line indicates known interactions from curated databases, a purple line indicates known interactions experimentally determined, a green line indicates gene neighborhood, a red line indicated gene fusions, a blue line indicates gene co-occurrence, a yellow line indicates text mining, a black line indicates co-expression, a light purple line indicates protein homology. The full name of the protein is shown in [Supplementary Table 2](#).



## ACKNOWLEDGMENTS

This study was supported by National Natural Science Foundation of China (31972137), China Agriculture Research System (CARS-41), Primary Research & Development Plan of Jiangsu Province (BE2017392), the Priority Academic Program Development of Jiangsu Higher Education Institutions, Overseas Expertise Introduction Center for Discipline Innovation (111 Center) On Quality & Safety Control and Nutrition of Muscle Food (B14023).

## SUPPLEMENTARY DATA

Supplementary data associated with this article can be found in the online version at <https://doi.org/10.1016/j.psj.2021.101029>.

## DISCLOSURES

The authors declare no conflicts of interest.

## REFERENCES

- Adibhatla, R. M., and J. F. Hatcher. 2006. Phospholipase A<sub>2</sub>, reactive oxygen species, and lipid peroxidation in CNS pathologies. *BMB Rep.* 41:560–567.
- Amaral, A. B., M. V. da Silva, and S. C. S. Lannes. 2018. Lipid oxidation in meat: mechanisms and protective factors - a review. *Food Sci. Technol.* 38:1–15.
- Benhar, M. 2018. Roles of mammalian glutathione peroxidase and thioredoxin reductase enzymes in the cellular response to nitrosative stress. *Free Radic. Biol. Med.* 127:160–164.
- Bolumar, T., M. L. Andersen, and V. Orlien. 2014. Mechanism of radical formation in beef and chicken meat during high pressure processing evaluated by electron spin resonance detection and the addition of antioxidants. *Food Chem.* 150:422–428.
- Burk, R. F., K. E. Hill, and A. K. Motley. 2003. Selenoprotein metabolism and function: evidence for more than one function for selenoprotein p. *J. Nutr.* 133:1517S.
- Chen, T., G. Zhou, X. Xu, G. Zhao, and C. Li. 2010. Phospholipase A<sub>2</sub> and antioxidant enzyme activities in normal and processed pork. *Meat Sci.* 84:143–146.
- Christopher, K. L., M. G. Pedler, B. Shieh, D. A. Ammar, J. M. Petrash, and N. H. Mueller. 2014. Alpha-crystallin-mediated protection of lens cells against heat and oxidative stress-induced cell death. *Biochim. Biophys. Acta Mol. Cell Res.* 1843:309–315.
- Chutkow, W. A., and R. T. Lee. 2011. Thioredoxin regulates adipogenesis through thioredoxin-interacting protein (txnip) protein stability. *J. Biol. Chem.* 286:29139–29145.
- DomÁnguez, R., M. Pateiro, M. Gagaoua, F. J. Barba, W. Zhang, and J. M. Lorenzo. 2019. A comprehensive review on lipid oxidation in meat and meat products. *Antioxidants* 8:429.
- Grunwald, E. W., and M. P. Richards. 2006. Studies with myoglobin variants indicate that released heme is the primary promoter of lipid oxidation in washed fish muscle. *J. Agri. Food Chem.* 54:4452–4460.
- Guyon, C., A. Meynier, and M. Lamballerie. 2016. Protein and lipid oxidation in meat: a review with emphasis on high-pressure treatments. *Trends Food Sci. Tech.* 50:131–143.
- Jurie, C., C. M. Bonnet, C. Leroux, D. Bauchart, P. Boulesteix, D. W. Petrick, and J. F. Hocquette. 2007. Adipocyte fatty acid-binding protein and mitochondrial enzyme activities in muscles as relevant indicators of marbling in cattle. *J. Anim. Sci.* 85:2660–2669.
- Kalmar, B., and L. Greensmith. 2009. Induction of heat shock proteins for protection against oxidative stress. *Adv. Drug Deliver. Rev.* 61:310–318.
- Kang, Y., M. Hu, Y. Zhu, X. Gao, and M. Wang. 2009. Antioxidative effect of the herbal remedy qin huo yi hao and its active component tetramethylpyrazine on high glucose-treated endothelial cells. *Life Sci.* 84:428–436.
- Karp, N. A., W. Huber, P. G. Sadowski, P. D. Charles, S. V. Hester, and K. S. Lilley. 2010. Addressing accuracy and precision issues in iTRAQ quantitation. *Mol. Cell. Proteomics* 9:1885–1897.
- Liu, Y., X. L. Xu, and G. H. Zhou. 2006. Changes in taste compounds of duck during processing. *Food Chem.* 102:22–26.
- Lu, J., and A. Holmgren. 2014. The thioredoxin antioxidant system. *Free Radic. Biol. Med.* 66:75–87.
- Mentzer, E. V., F. L. Zhang, and J. A. Hamilton. 2001. Binding of 13-hode and 15-hete to phospholipid bilayers, albumin, and intracellular fatty acid binding proteins. *J. Biol. Chem.* 276:15575–15580.
- Meullenet, J., E. Jonville, D. Grezes, and C. M. Owens. 2004. Prediction of the texture of cooked poultry pectoralis major muscles by near-infrared reflectance analysis of raw meat. *J. Texture Stud.* 35:573–585.
- Murrant, C. L., and M. B. Reid. 2001. Detection of reactive oxygen and reactive nitrogen species in skeletal muscle. *Microsc. Res. Techniq.* 55:236–248.
- Murali, M., M. S. Carvalho, and T. Shivanandappa. 2020. Oxidative stress-mediated cytotoxicity of endosulfan is causally linked to the inhibition of NADH dehydrogenase and Na<sup>+</sup>, K<sup>+</sup>-ATPase in Ehrlich ascites tumor cells. *Mol. Cell. Biochem.* 468:59–68.
- Pamplona, R. 2008. Membrane phospholipids, lipoxidative damage and molecular integrity: a causal role in aging and longevity. *Biochim. Biophys. Acta* 1777:1249–1262.
- Pelin, M., L. Fusco, C. Martin, S. Sosa, J. Frontián-Rubio, J. M. Gonzalez-Dominguez, M. Duran-Prado, E. Vazquez, M. Prato, and A. Tubaro. 2018. Graphene and graphene oxide induce ROS production in human HaCaT skin keratinocytes: the role of xanthine oxidase and NADH dehydrogenase. *Nanoscale* 10:11820–11830.
- Ronsein, G. E., N. Pamir, P. D. von Haller, D. S. Kim, M. N. Oda, G. P. Jarvik, T. Vaisar, and J. W. Heinecke. 2015. Parallel reaction monitoring (PRM) and selected reaction monitoring (SRM) exhibit comparable linearity, dynamic range and precision for targeted quantitative HDL proteomics. *J. Proteomics* 0:388–399.
- Sayd, T., C. Chambon, E. Laville, B. Lebret, H. Gilbert, and P. Gatellier. 2012. Early post-mortem sarcoplasmic proteome of porcine muscle related to lipid oxidation in aged and cooked meat. *Food Chem.* 135:2238–2244.
- Sorensen, G., and S. S. Jorgensen. 1996. A critical examination of some experimental variables in the 2-thiobarbituric acid (TBA) test for lipid oxidation in meat products. *Z. Lebensm. Unters. Forsch.* 202:205–210.
- Tatibayorworntham, N., and M. P. Richards. 2015. Effects of phospholipase A<sub>2</sub> on lipid oxidation in pork, poultry, and fish. *Meat Sci.* 101:159–160.
- Tsuchiya, H., K. Tanaka, and Y. Saeki. 2013. The parallel reaction monitoring method contributes to a highly sensitive polyubiquitin chain quantification. *Biochem. Biophys. Res. Commun.* 436:223–229.
- Tsvetkova, N. M., I. Horváth, Z. Török, W. F. Wolkers, Z. Balogi, N. Shigapova, L. M. Crowe, F. Tablin, E. Vierling, J. H. Crowe, and L. VÁgh. 2002. Small heat-shock proteins regulate membrane lipid polymorphism. *Proc. Natl. Acad. Sci. U. S. A.* 99:13504–13509.
- Wang, D., W. Xu, X. Xu, G. Zhou, Y. Zhu, C. Li, and M. Yang. 2009. Determination of intramuscular phospholipid classes and molecular species in gaoyou duck. *Food Chem.* 112:150–155.
- Wu, H., J. Yin, J. Zhang, and M. P. Richards. 2017. Factors affecting lipid oxidation due to pig and Turkey hemolysate. *J. Agri. Food Chem.* 65:8011–8017.
- Xiao, L., Z. Xin, G. P. Zhou, C. X. Wu, C. Li, and X. H. Xu. 2017. Electroacupuncture reduces apoptotic index and inhibits p38 mitogen-activated protein kinase signaling pathway in the hippocampus of rats with cerebral ischemia/reperfusion injury. *Neural Regen. Res.* 12:409–416.
- Zhang, M., D. Wang, P. Li, C. Sun, R. Xu, Z. Geng, W. Xu, and Z. Dai. 2018a. Interaction of hsp90 with phospholipid model membranes. *Biochim. Biophys. Acta Biomembr.* 1860:611–616.
- Zhang, M., D. Wang, Z. Geng, P. Li, Z. Sun, and W. Xu. 2018b. Effect of heat shock protein 90 against ROS-induced phospholipid oxidation. *Food Chem.* 240:642–647.
- Zoidis, E., I. Seremelis, N. Kontopoulos, and G. P. Danezis. 2018. Selenium-dependent antioxidant enzymes: actions and properties of selenoproteins. *Antioxidants* 7:26.